Organic Geochemistry 139 (2020) 103946

Contents lists available at ScienceDirect

Organic Geochemistry

journal homepage: www.elsevier.com/locate/orggeochem

Two new isoprenoidal ketones related to *Botryococcus braunii* in the Chinese Maoming Basin

Jing Liao [a,1], Xiangyun Zhang [a,1], Hong Lu [a,*], Youping Zhou [b,*], Quan Shi [c], Ping'an Peng [a], Guoying Sheng [a]

[a] State Key Laboratory of Organic Geochemistry, Guangzhou Institute of Geochemistry and Institutions of Earth Science, Chinese Academy of Sciences, Guangzhou 510640, China
[b] Isotopomics in Chemical Biology & Shaanxi Key Laboratory of Chemical Additives for Industry, School of Chemistry & Chemical Engineering, Shaanxi University of Science & Technology, Xi'an 710021, China
[c] State Key Laboratory of Heavy Oil Processing, China University of Petroleum, Beijing 102249, China

ARTICLE INFO

Article history:
Received 30 June 2019
Received in revised form 19 October 2019
Accepted 23 October 2019
Available online 31 October 2019

Keywords:
Shortened oxygenated botryococcenoids
Chinese Maoming basin
NMR spectroscopy
Pathway

ABSTRACT

We report the spectroscopy-based (NMR, HRMS, IR) reassignment of the structures of two previously mis-identified saturated methyl ketones (formerly C_{15} ketone: *5,9-dimethyl-6-isopropyl-2-decanone* and C_{18} ketone: *4,9,11-trimethyl-6-isopropyl-2-dodecanone*) in the Maoming oil shale to: *5,6,9,10-tetramethy lundecan-2-one* and *4,7,8,11,12-pentamethyltridecan-2-one,* respectively.

A diagenetic pathway is proposed to explain the isotopic and structural closeness between these two methyl ketones and recently identified saturated C_{31} alcohols, C_{32} aldehydes and C_{33} ketones (all with a unique methyl group β to the sole quaternary carbon in their skeletons) obtained from the same Maoming Basin sediments. The pathway involves, firstly, epoxidation, hydration, oxidation and double decarboxylation of the C_{33} botryococcene to C_{31} botryococcene. Subsequent photo- or autoxidation of the internal double bond around the quaternary carbon in the C_{31} botryococcene in an oxic environment leads to the formation of a C_{31} hydroperoxy-alkene. A heterolytic (Hock-type) or homolytic cleavage of the hydroperoxy-alkene around the quaternary carbon then gives rise to the C_{15} and C_{18} unsaturated methyl ketones, respectively. The so-formed unsaturated ketones are then geochemically stabilized by hydrogenation in an anoxic environment.

1. Introduction

In 2017, we (mis)identified two oxygenated isoprenoids (a C_{15} ketone *5,9-dimethyl-6-isopropyl-2-decanone* and a C_{18} ketone *4,9,11-trimethyl-6-isopropyl-2-dodecanone:* Zhang et al., 2017, now retracted) from the polar fraction of a Maoming oil shale extract, based on nuclear magnetic resonance (NMR) spectroscopy and mass spectrometric (MS) analyses. The extract also contained abundant botryococcanoid biomarkers, presumably produced by B race *Botryococcus braunii* (*B. braunii*) (Brassell et al., 1986). More recently, from the same sample, we identified, based on a combination of preparative gas chromatography (pGC), NMR spectroscopy, MS and Lindeman and Adams modelling of the ^{13}C chemical shifts (Lindeman and Adams, 1976), a group of oxygenated botryococcanoids in the carbon number range of C_{31}–C_{33}: a C_{33} botryococcan-24-one, undecamethylhenicosanal (C_{32} UMH-al), and two C_{31} decamethylheneicosanols (C_{31} DMH-ol), in addition to a group of botryococcanes (two 2,3,6,7,10,12,15,16,19,20-deca methylhenicosanes: C_{31} DMHs; 2,3,6,7,10,10,12,15,16,19,20-unde camethylhenicosane: C_{32} UMH; C_{33} botryococcane), all with a unique skeleton where a methyl group is positioned β to the sole quaternary carbon (Liao et al., 2018a, 2018b, 2019, under review) (Fig. 1).

Since the carbon isotopic compositions of these two groups of compounds with different assigned skeletons are similar (the $\delta^{13}C$ values of the C_{15} and C_{18} ketones are −8.5‰ and −8.7‰ V-PDB, respectively, while those for C_{31}, C_{32} and C_{33} botryococcanes are −7.4, −7.6‰, −8.7‰ and −8.5‰ V-PDB, respectively) and since they were found in the same oil shale sample, we suspect they are genetically related. If this genetic relationship exists, it is highly likely that the latter group is the precursor of the former as the B race *B. braunii* is known to produce botryococcenes in the carbon range of C_{30-37}, and therefore shares part of the skeleton with the former. This prompted us to re-examine the NMR and MS

* Corresponding authors at: State Key Laboratory of Organic Geochemistry, Guangzhou Institute of Geochemistry and Institutions of Earth Science, Chinese Academy of Sciences, 511 Kehua Street, Tianhe District, Guangzhou 510640, China (H. Lu). Isotopomics in Chemical Biology, School of Chemistry & Chemical Engineering, Shaanxi University of Science & Technology, Weiyang University Park, Xi'an 710021, China (Y. Zhou).

E-mail addresses: luhong@gig.ac.cn (H. Lu), youping.zhou@sust.edu.cn (Y. Zhou).

[1] Equal contributors.

https://doi.org/10.1016/j.orggeochem.2019.103946
0146-6380/

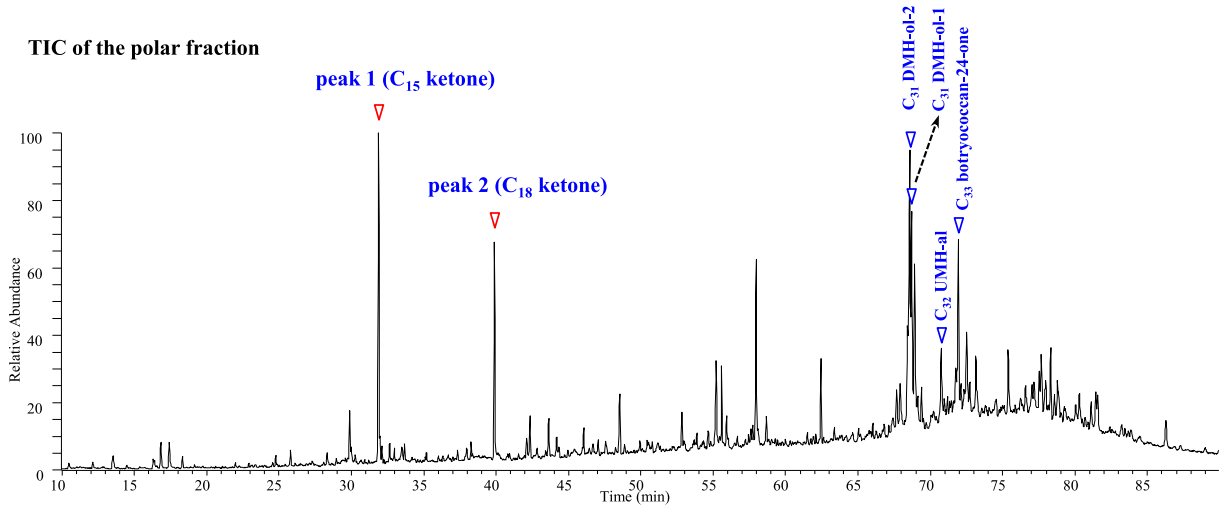

Fig. 1. TIC (total ion current, a) of the polar fraction of the extract from a sediment sample collected from Maoming Basin. The GC oven was programmed from 80 °C (held for 2 min) to 295 °C at a rate of 3 °C/min, and held for 25 min.

evidence on which we based our original structure assignment of these two ketones. In this submission, we report and redress the deficiency of our previous identification by comparing the measured and Lindeman & Adam modeled ^{13}C chemical shifts, in addition to the 2D-NMR spectra, HRMS and IR analyses. The comparison leads to the conclusion that the two compounds were, as suspected, the geochemical offspring of the C_{31-33} botryococcenes.

2. Material and methods

2.1. Isolation and purification

The sample was collected from the Eocene oil-shale formation in the Chinese Maoming Basin (further details appear in Liao et al., 2018a, 2018b). It was ground to 100 mesh and Soxhlet-extracted with CH_2Cl_2/CH_3OH (9:1, v/v) for 72 h. Activated Cu filings were used to remove elemental sulfur. The asphaltene fraction was removed centrifugally from the extracts by precipitation in *n*-hexane. The saturated, aromatic and polar fractions were eluted on silica/aluminium oxide column chromatography, with *n*-hexane (80 mL), *n*-hexane/dichloromethane (3:2, v/v, 50 mL) and methanol (30 mL) in sequence. The polar fraction was further separated into three sub-fractions.

The target compounds (peaks 1 and 2 in Fig. 1) were eluted in the polar sub-fraction (N3) with CH_2Cl_2/*n*-hexane (1:1, v/v, 40 mL), which was next subjected to PGC (Zuo et al, 2013) on an Agilent 7890 gas chromatograph interfaced to a Gerstel-preparative fraction collector (PFC), similar to that described by Eglinton et al. (1996). Helium (purity 99.999%) with a constant 3.0 mL/min flow was used as the carrier gas for separations through a DB-5 column (60 m × 0.53 mm × 1.5 μm film thickness). The column temperature was held at 80 °C for 2 min, programmed to 210 °C at 3 °C/min, and then to 300 °C at 30 °C/min, and held for 15 min at 300 °C.

About 1.0 mg of the compound peak 1 and 0.7 mg of the compound peak 2 were collected. The purity was confirmed by GC/MS and GC/FID analysis as greater than 95% (Figs. S1 and S2). The purified target compounds were then subjected to NMR spectral analysis for structural assignments.

2.2. Instrumental analysis

Gas chromatography-high resolution electron impact mass spectrometry (GC/HREIMS) was performed on a Thermo Finnigan MAT95XP mass spectrometer (Germany) to determine the accurate mass. The HRMS system was operated in the electron ionization mode (42 eV) at a resolution of R > 10,000 (10% valley). FT-IR analyses were conducted on a FT-IR Tenor 27 spectrophotometer (Bruker Corporation, Billerica, USA) with the sample loaded as a KBr pellet. The spectrometer was operated in an absorption mode in the wavenumber range of 475 cm^{-1} to 3675 cm^{-1} at a resolution of 2 cm^{-1}.

GC/EIMS analysis was performed on a Trace Ultra GC interfaced with a Thermo DSQ-II mass spectrometer operating at 70 eV with a mass range of *m/z* 50–650. A HP-5 column (30 m × 0.25 mm × 0.25 μm film thickness) was used. The oven temperature program is described in the figure legend. Helium (purity 99.999%) was used as the carrier gas with a constant 1.2 mL/min flow mode.

^1H and ^{13}C NMR spectra were acquired on a Bruker AVANCE III 400 MHz NMR spectrometer (operating at 400 MHz for ^1H NMR spectra and 100 MHz for ^{13}C NMR spectra). Spectra were recorded in $CDCl_3$ solutions, with TMS as the internal standard. Chemical shifts in the ^1H NMR spectra were referenced relative to the residual proton signal (7.26 ppm) while ^{13}C NMR spectral chemical shifts were referenced to the central line of ^{13}C multiplet (77.0 ppm) of $CDCl_3$. A combination of ^{13}C spectrum and distortionless enhanced polarization transfer (DEPT) spectra (DEPT 90° and 135°) were acquired to determine the multiplicity of each ^{13}C nucleus. 1D, 2D heteronuclear (heteronuclear multiple bond correlation: HMBC; heteronuclear single quantum correlation: HSQC) and homonuclear (^1H–^1H correlation spectroscopy: COSY) NMR spectral analysis were used to assign the individual resonances.

3. Results and discussion

3.1. Structural assignment for the C_{15} and C_{18} ketones

In the TIC chromatogram (total ion current, Fig. 1), the C_{15} and C_{18} ketones were readily identified as the major components in the polar fraction of the Maoming sediment extracts. These two ketones eluted earlier than the C_{31} alcohols, C_{32} aldehyde and C_{33} ketones, each with a unique β-positioned methyl group in their skeletons (Liao et al., 2019, under review).

C_{15} ketone (*5,6,9,10-tetramethyl-undecan-2-one*). HREIMS analysis showed that peak 1 (the C_{15} ketone) had an accurate mass

Table 1
^{1}H (400 MHz) and ^{13}C (100 MHz) NMR spectra data of the C_{15}-ketone measured in $CDCl_3$.

Position	^{1}H, δ (ppm), Multiplicity (*J* in Hz)	^{13}C, δ (ppm), multiplicity	DEPT	HMBC ($^{1}H \rightarrow {}^{13}C$)	^{1}H-^{1}H COSY cross peaks
1	2.15, s	29.8, q	CH_3		
2		209.6, s	C	1, 3	
3	2.37, m; 2.48, m	42.3, t	CH_2	1	1.32, 1.63
4	1.37, overlap; 1.63, m	26.7, t	CH_2	12	1.37, 2.37, 2.48
5	1.37, overlap	37.1, d	CH	3, 13	0.83, 1.63
6	1.34, overlap	38.1, d	CH	12	0.83
7	0.97, overlap; 1.35, overlap	30.8, t	CH_2	13	0.96, 1.35
8	0.96, overlap; 1.35, overlap	32.3, t	CH_2	14	0.97, 1.35
9	1.24, overlap	38.9, d	CH	10, 11, 14, 15	0.78, 1.57
10	1.57, m	31.6, d	CH		0.78, 0.85, 1.24
11	0.85, d (6.8)	20.4, q	CH_3	10, 15	1.57
12	0.83, d (6.3)	16.3, q	CH_3		1.37
13	0.83, d (6.8)	16.3, q	CH_3		1.34
14	0.78, d (6.8)	15.3, q	CH_3	10	1.24
15	0.78, d (6.8)	17.6, q	CH_3	10, 11	1.57

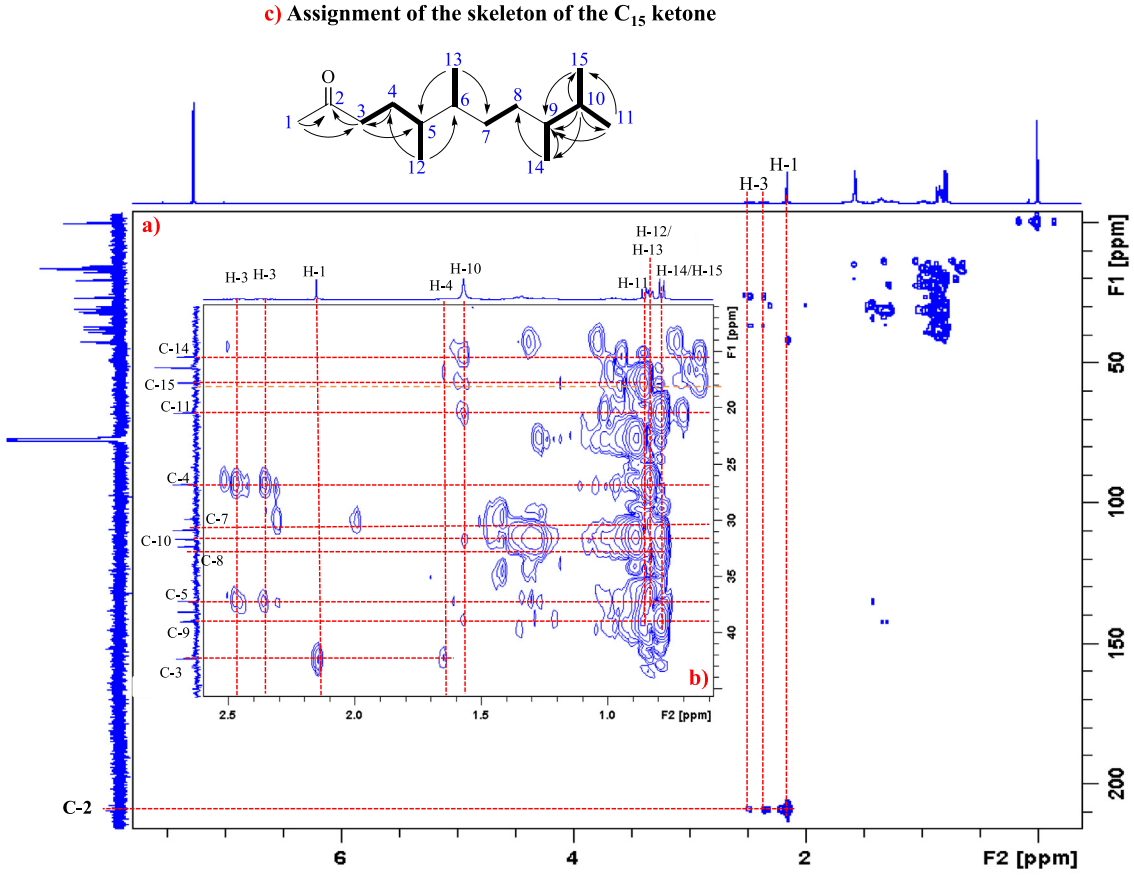

Fig. 2. ^{1}H-^{13}C HMBC spectrum (a & b) and key ^{1}H-^{1}H COSY (bold bond) and HMBC correlations ($^{1}H \rightarrow {}^{13}C$) for the skeleton of the new C_{15} ketone (c). The blue numbers in 2c are for the labelling of the carbons in the skeleton. (For interpretation of the references to colour in this figure legend, the reader is referred to the web version of this article.)

of 226.2291 (Fig. S3), in close agreement with the calculated mass of 226.2297 for $C_{15}H_{30}O$, indicating one degree of unsaturation. In the FT-IR spectrum (Fig. S5), there was an absorption band at 1716 cm^{-1} typical of that due to a C=O group (Mösle et al., 1998) and no absorptions between 2820 and 2850 & 2720–2750 cm^{-1} characteristic of the C—H stretching vibration of an aldehyde group, indicating that the unsaturation derived from a keto rather than from an aldehyde functional group.

1D and 2D-NMR spectral data for the C_{15} ketone are summarized in Table 1 and can be found in Figs. S7–S11. The ^{13}C NMR spectrum (Fig. S8) contained 14 resonances which can be ascribed to 1C, 4 CH, 4 CH_2 and 6 CH_3 according to the DEPT experiments. Since the δ_C 16.3 ppm represented the overlapping resonances of two CH_3 groups, there are a total of 15 carbons, consistent with the HREIMS-based formula $C_{15}H_{30}O$. The 2D-NMR spectra-based structural assignment (see Figs. S9–S11, 2, Table 1 for the chemical shift data and spectra) of the C_{15} ketone was conducted as follows.

The chemical shift of 209.6 ppm in the HMBC spectrum (Fig. 2a) indicates the presence of a carbonyl carbon (Aasen et al., 1976), which is corroborated by the absorption band (1716 cm^{-1}) in the IR spectrum. The HMBC correlation of the singlet of H-1 to the carbonyl carbon C-2 implied a C-1/C-2 connection, which is

consistent with the δ_C at 29.8 ppm for a CH_3 (C-1) deshielded by the neighbouring carbonyl group (Breitmaier and Voelter, 1978; Cheng and Bennett, 1991; Cheng, 1994). HMBC correlations (Fig. 2a, b) from H-3 to C-2 and H-1 to C-3 indicated a C-2/C-3 connection. Connections C-3/C-4, C-5/C-12 and C-6/C-13 were established by cross peaks (bold bonds in Fig. 2c) in ^{1}H-^{1}H COSY spectrum between H-3 and H-4, H-5 and H-12, and H-6 and H-13 (Fig. S10). The HMBC correlations from H-3 to C-5 and H-12 to C-4 indicates the C-4/C-5 connection, the correlations between H-12 to C-6 and H-13 to C-5 showed a C-5/C-6 connection while those correlations (Fig. 2b) from H-13 to C-7 and cross peak (bold bonds in Fig. 2c) between H-7 and H-8 indicated the C-6/C-7 and C-7/C-8 connections. The HMBC spectrum (Fig. 2b) also established the connections C-9/C-10, C-10/C-11, C-9/C-14, and C-10/C-15 by correlations (Fig. 2b) from H-10, H-11, H-14 and H-15 to C-9, and H-11 to C-15 (see Fig. S10 for the COSY spectrum for the correlations between H-9 & H-14, H-9 & H-10, H-10 & H-11 and H-10 & H-15). HMBC correlation (Fig. 2b) from H-14 to C-8 indicates the connection between the substructure (C-9 to C-11) and C-8. Accordingly, the C_{15} ketone was identified as 5,6,9,10-tetramethylundecan-2-one (Fig. 2c).

The mass spectrum (Fig. 4a) of the C_{15} ketone displayed a molecular ion at *m/z* 226, in accordance with the results of HREIMS analysis. The base peak *m/z* 71 and the major peak *m/z* 99 correspond to the loss of C_5H_{11} and C_7H_{15} from C-8/C-9 and C-6/C-7 fissions, respectively (Fig. 4a). The ion at *m/z* 168 [M^+-58] is consistent with the theoretical prediction for a loss of acetone (Liao et al., 2018b). The characteristic ion at *m/z* 208 [M^+-18] is likely to result from the loss of the ketone-O in the form of a H_2O following a hydrogen transfer (Fig. 4a).

C_{18} ketone (*4,7,8,11,12-pentamethyl-tridecan-2-one*). The HREIMS analysis of the C_{18} ketone showed an accurate mass of 268.2760 (Fig. S4), which was in agreement with a calculated accurate mass of 268.2766 for a formula of $C_{18}H_{36}O$, indicating one degree of unsaturation. An absorption band at 1716 cm^{-1} and absence of absorptions between 2820–2850 & 2720–2750 cm^{-1} in the FT-IR spectrum (Fig. S6) indicated the unsaturation is from a ketone rather than from an aldehyde. 1D and 2D-NMR spectra data for the C_{18} ketone are summarized in Table 2 and can be found in Figs. S12–S16. 1D ^{13}C spectrum, DEPT 90°, 135° and 2D HMBC spectrum (Figs. S13 and 3) show that there are 7 CH_3, 5 CH_2, 5 CH and 1C, consistent with the $C_{18}H_{36}O$ inferred from HREIMS analysis.

2D-NMR spectra-based structural assignment for this C_{18} ketone was conducted in a similar way to those conducted for the C_{15} ketone (see Figs. S13–S16 and Table 2 for the 2D-NMR spectra data).

Again the resonance at 209.6 ppm in the HMBC (Fig. 3a) spectrum indicates the presence of a carbonyl carbon. The correlation from H-1 to carbonyl carbon C-2 indicates a C-1/C-2 connection, consistent with the IR spectrum showing a ketone carbonyl group. HMBC correlation (Fig. 3b) from H-1 to C-3 showed the connection C-2/C-3. The δ_C at 30.4 ppm and δ_H at 2.13 for C-1 (CH_3) are consistent with the C-1 being deshielded by the

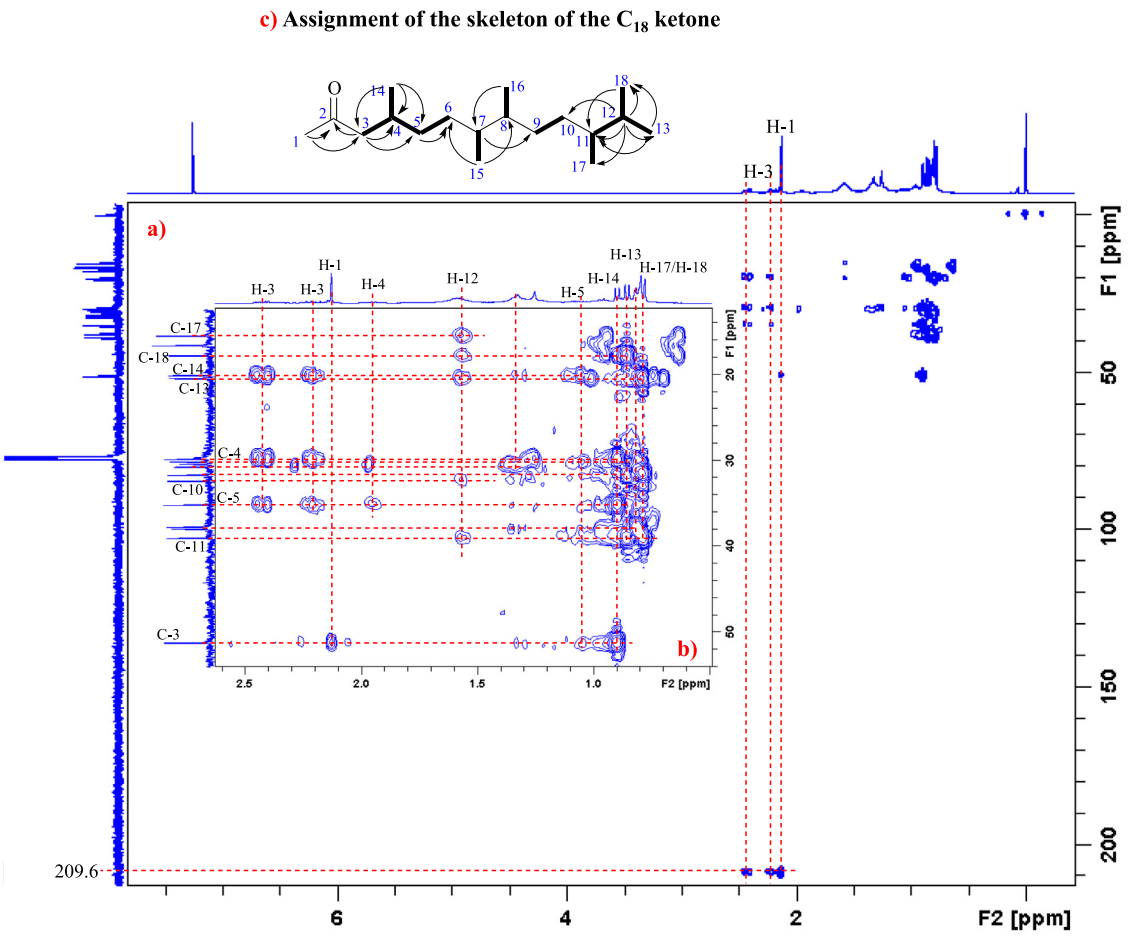

Fig. 3. ^{1}H-^{13}C HMBC spectrum (a & b) and key ^{1}H-^{1}H COSY (bold bonds) and HMBC correlations (^{1}H → ^{13}C) for the skeleton of the new C_{18} ketone (c). The blue numbers in (c) are for the labelling of the carbons in the skeleton. (For interpretation of the references to colour in this figure legend, the reader is referred to the web version of this article.)

a) peak-1($C_{15}H_{30}O$: *5,6,9,10-tetramethylundecan-2-one*)

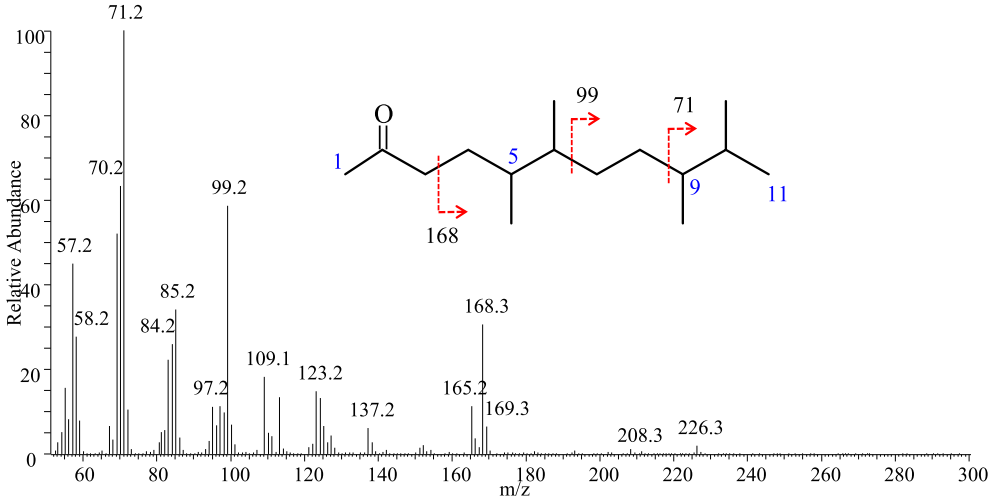

b) peak-2 ($C_{18}H_{36}O$: *4,7,8,11,12-pentamethyltridecan-2-one*)

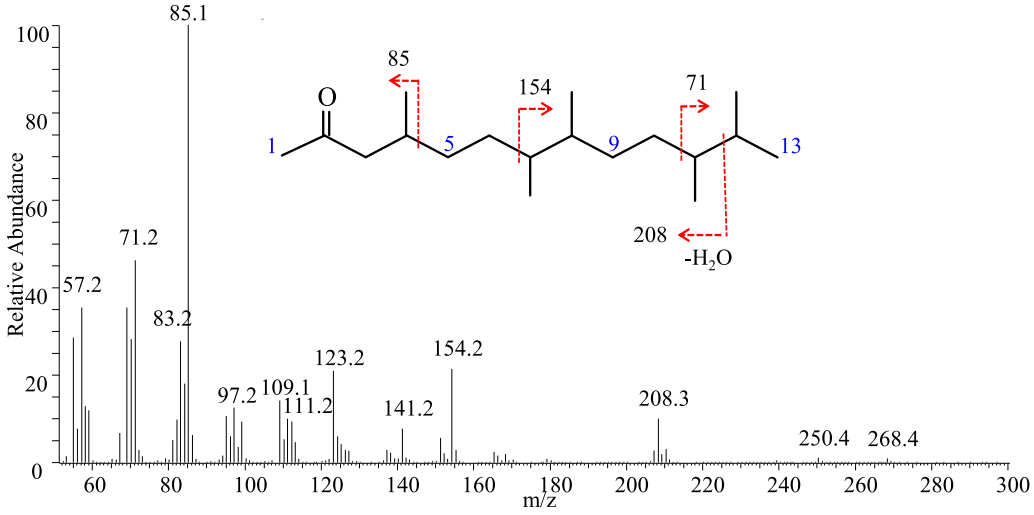

Fig. 4. Interpretation of the mass spectra of the C_{15} (a) and C_{18} (b) ketones.

Table 2
^{1}H (400 MHz) and ^{13}C (100 MHz) NMR spectra data of the C_{18}-ketone measured in $CDCl_3$.

Position	^{1}H, δ (ppm), Multiplicity (*J* in Hz)	^{13}C, δ (ppm), multiplicity	DEPT	HMBC ($^{1}H \rightarrow {}^{13}C$)	^{1}H-^{1}H COSY cross peaks
1	2.13, s	30.4, q	CH_3		
2		209.6, s	C	1, 3	
3	2.23, m; 2.43, m	51.2, t	CH_2	1, 14	1.95
4	1.95, m	29.6, d	CH	1, 3	0.90, 1.07, 1.30, 2.23, 2.43
5	1.07, m; 1.30, overlap	35.1, t	CH_2	3, 4, 14	1.95, 1.25
6	1.25, overlap	30.1, t	CH_2	5, 15	1.30
7	1.31, overlap	37.9, d	CH	16	0.81
8	1.32, overlap	37.7, d	CH	15	0.82
9	0.95, overlap; 1.35, overlap	30.7, t	CH_2	7	0.97, 1.32
10	0.97, overlap; 1.32, overlap	32.3, t	CH_2	12	0.95, 1.35
11	1.21, m	38.9, d	CH	12, 13, 18	0.79, 1.57
12	1.57, m	31.6, d	CH	13	0.79, 0.86, 1.21
13	0.86,d (6.8)	20.4, q	CH_3	12, 18	1.57
14	0.90,d (6.6)	20.0, q	CH_3	3	1.95
15	0.81, d (6.4)	16.3, q	CH_3		1.31
16	0.82,d (6.4)	16.3, q	CH_3		1.32
17	0.79, d (6.8)	15.4, q	CH_3	12	1.21
18	0.79, d (6.8)	17.3, q	CH_3	12, 13	1.57

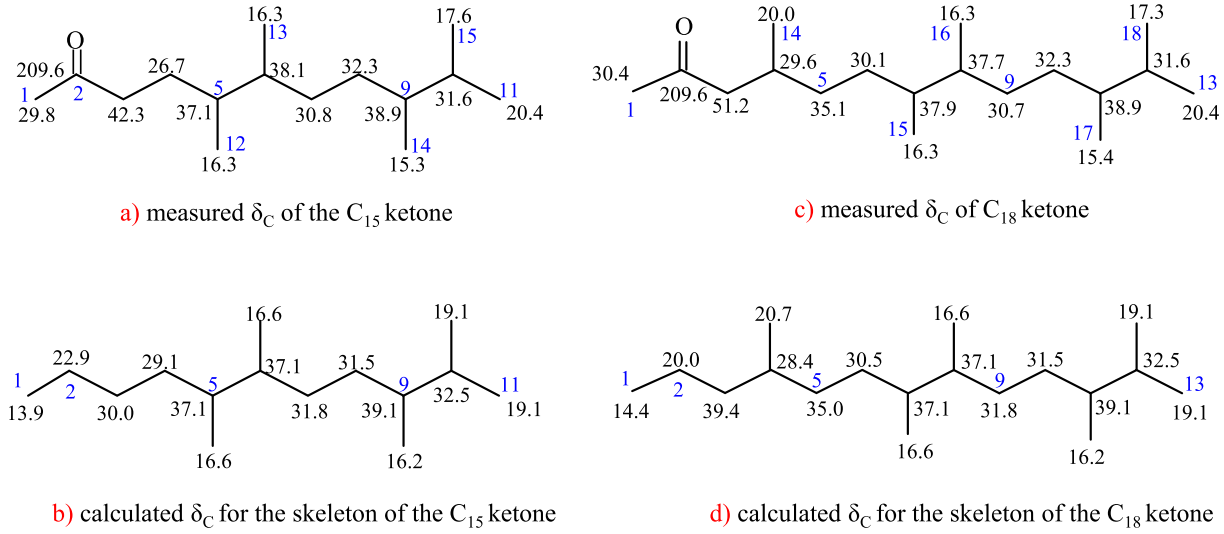

Fig. 5. Measured (a and c) and modeled (b and d) δ_C values for the new C_{15} and C_{18} ketones. The numbers in blue are for the labelling of the carbon in the new skeletons while those in black are for carbon chemical shifts. (For interpretation of the references to colour in this figure legend, the reader is referred to the web version of this article.)

neighbouring carbonyl group (Breitmaier and Voelter, 1978; Cheng and Bennett, 1991; Cheng, 1994). The HMBC spectrum (Fig. 3b) established the connections C-3/C-4, C-4/C-5, and C-4/C-14 by correlations from H-14 to C-3, C-4, and C-5. Other HMBC correlations from H-3 to C-4 and C-5 and cross peaks (bold bonds in Fig. 3c) in the ^{1}H-^{1}H COSY spectrum between H-3 and H-4, H-4 and H-14, H-4 and H-5 confirmed the three connections (Fig. S15). Cross peaks in the ^{1}H-^{1}H COSY spectrum (Fig. S15) between H-5 and H-6, H-7 and H-15, H-8 and H-16 indicated the connections C-5/C-6, C-7/C-15, and C-8/C-16 (Fig. 3c). The HMBC experiment (Fig. 3b, c) further established the connections C-6/C-7, C-7/C-8, and C-8/C-9 by correlations from H-15 to C-6, H-15 to C-8, H-16 to C-7, and H-7 to C-9. Cross peaks in the ^{1}H-^{1}H COSY spectrum (Fig. S15) between H-9 and H-10 indicated the connection C-9/C-10. The HMBC spectrum (Fig. 3b) established the connections C-11/C-12, C-12/C-13, C-11/C-17, and C-13/C-18 by correlations (Fig. 3b) from H-12, H-13, H-17 and H-18 to C-11, and H-13 to C-18 (see the Fig. S15 for the COSY spectrum for the correlations between H-11 & H-17, H-11 & H-12, H-12 & H-13 and H-12 & H-18). HMBC correlation (Fig. 3b) from H-12 to C-10 connected C-10 indicates that C-11 is connected to C-10. Accordingly, the C_{18} ketone was assigned as 4,7,8,11,12-pentamethyl-tridecan-2-one (Fig. 3c).

The molecular ion, *m/z* 268, in the mass spectrum (Fig. 4b) of the C_{18} ketone is consistent with the inferred formula of $C_{18}H_{36}O$ from HREIMS analysis. The major ion at *m/z* 154 [M^+-58-56] is interpreted as resulting from a loss of the fragment C-1 ~ C-6 following a McLafferty rearrangement. The characteristic ion at *m/z* 250 [M^+-18] was likely to result from the loss of the ketone-O in the form of H_2O following a hydrogen transfer, while *m/z* 208 was likely to be a result of a further loss of the terminal propylene following the water loss.

To validate the assigned structures, the measured carbon chemical shifts (δ_C values) for the proposed new ketones (Fig. 5a, c) were compared with the calculated δ_C values of their corresponding alkanes following Lindeman and Adams modelling (Lindeman and Adams, 1971; Fig. 5b, d). The measured δ_C values for all carbons (except for the carbonyl carbon C-1 and those α- and β- to it which were deshielded by the carbonyl group, Fig. 5a, c) were very close to the calculated values (C-4 ~ C-15 for C_{15} alkane, C-4 ~ C-18 for C_{18} alkane, Fig. 5b, d). The discrepancies between the measured and calculated δ_C values of corresponding carbons were in most cases less than 1.0 ppm (Fig. 5), indicating the robustness of the structural assignments for the two new ketones.

3.2. Proposed pathway for the formation of the novel C_{15} ketone and C_{18} ketone.

Since the C_{15} and C_{18} ketones identified here clearly represent parts of the skeleton of the tertiary C_{31} DMH-ols identified in the same polar fraction as the two new methyl ketones (Liao et al., 2019, under review) and with their $\delta^{13}C$ also close to the latter, it is reasonable to assume that they are genetically related. In the shallow oxic lacustrine environment of the Maoming Basin, indicated by molecular and microscopic examination of the stratigraphic succession of the Maoming oil shale (Brassell et al., 1986), aerobic biodegradation (e.g. Deming and Baross, 1993; Hinrichs, 1993) and photo- and autoxidation (e.g. Wheeler, 1972; Rontani et al., 1987, 1988, 2011; Simoneit et al., 2009) of the botryococcenes seem likely pathways for their formation. As photo- and autoxidation of alkenes is known to lead to the formation of hydroperoxides (Frimer, 1979; Rontani et al., 2011, 2013), and homolysis and heterolysis (Hock cleavage) of the O—O bond in the hydroxyperoxide (Olah et al., 1976; Rontani, 2012; Rontani et al., 2013) can lead to the formation of ketones, we propose the following pathway (Fig. 6) to account for the presence of these two methyl ketones and their genetic relationships with the oxygenated botryococcene derivatives with the unique β-position methyl group (Liao et al., 2018a, 2018b).

The proposed pathway starts from the novel C_{33} botryococcene (**1**) (Fig. 6) formed from an unusual c1′-2-3-2′ condensation (cyclobutanation) of two farnesyl diphsophates (FPP) *in vivo* (Liao et al., 2018a). Following sequential epoxidation, hydration, oxidation and decarboxylation to produce the C_{32} botryococcenoic acid (**2**) (Liao et al., 2019, under review), C_{31} botryococcene (**3**), C_{31} botryococcenols (**11** and **12**), and C_{31} botryococcanols (**13** and **14**) are successively produced by decarboxylation (Bigley and Clarke, 1982), *syn*- or *anti*-addition of H_2O (Jin and Hanefeld, 2011; Resch and Hanefeld, 2015), hydrogenation and dehydration (Fig. 6). Photo-oxidation or auto-oxidation of **3** would produce the hydroperoxyalkene (**4**). A heterolytic (Hock type) or homolytic cleavage of **4** then leads to the corresponding C_{31} alkoxyl cation (**5**) or C_{31} alkoxyl radical (**6**), respectively. Cleavage α or β to the quaternary carbon gives C_{15} (**7**) and C_{18} (**8**) alkenyl ketones, respectively. Hydrogenation then stabilizes **7** and **8** as the C_{15} and C_{18} ketones (**9** and **10**) identified herein. Photo- or autoxidation of the central trisubstituted double

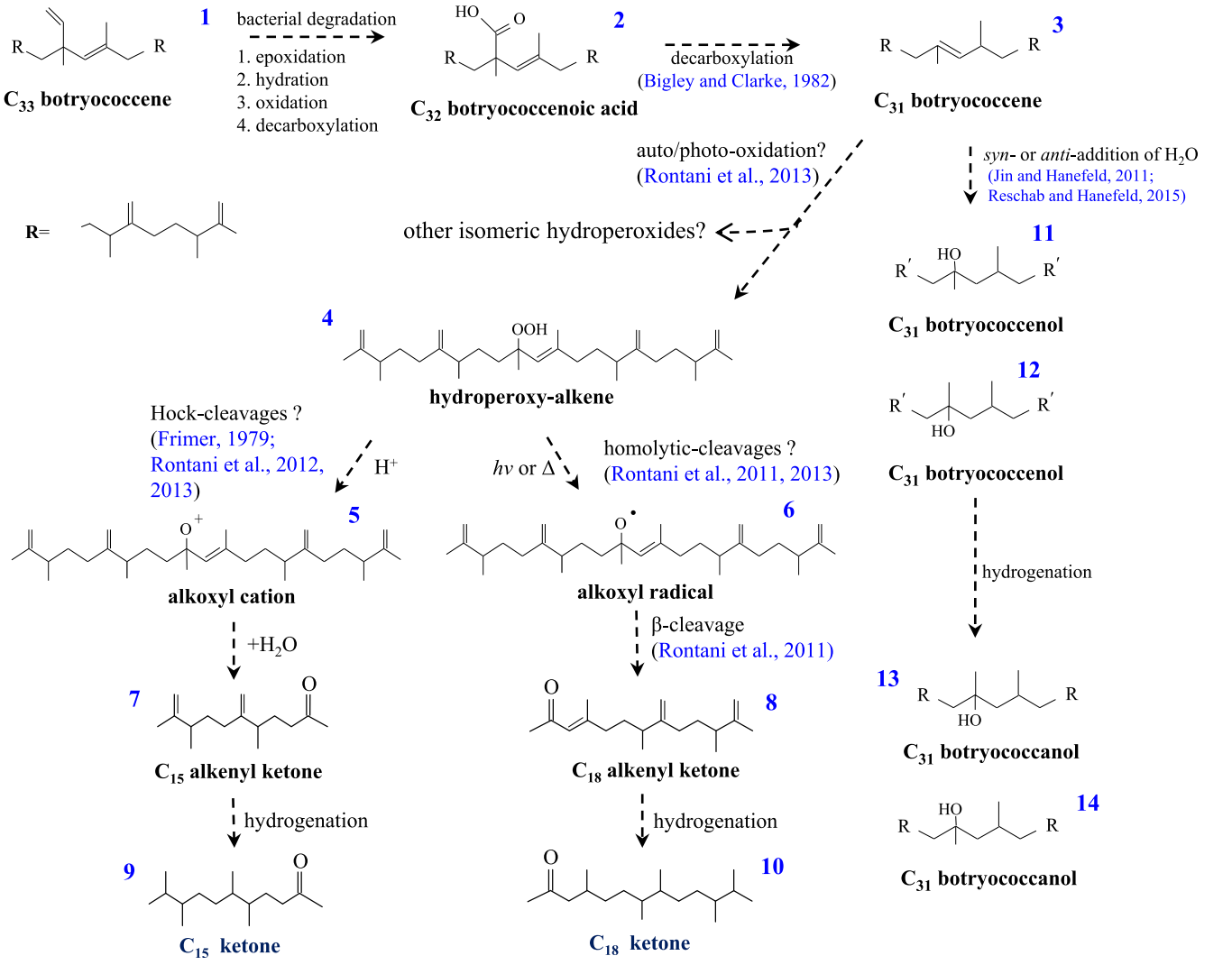

Fig. 6. Proposed pathways for the formation of the C_{15} and C_{18} ketones. *Cf* Liao et al., 2018a, 2018b, 2019, under review) for further details for the pathway leading to the synthesis of C_{33} botryococcene (1) and C_{32} botryococcenoic acid (2).

bond in the C_{31} botryococcene (**3**) might produce other isomeric hydroperoxides (Rontani et al., 2013), but none of these putative products have been found in our sample.

4. Conclusions

Degradation of botryococcenes synthesized by the B race *B. braunii* to produce short-chain oxygenated derivatives and altered skeletons is a likely geochemical pathway but has not been substantiated. This is due, at least in part, to the lack of rigor in the identification of compounds suspected to be the degradative products of the botryococcenes. Here, we redressed the deficiency in our previous identifications of two C_{15} and C_{18} ketones co-occurring with the C_{31}–C_{33} (oxygenated) botryococcanes with 2D-NMR spectroscopy, IR, HRMS and Lindeman & Adam chemical shift modelling. The C_{15} and C_{18} ketones were re-identified as 5,6,9,10-tetramethyl-undecan-2-one and 4,7,8,11,12-pentamethyl-tridecan-2-one, respectively.

Photo- or auto-hydroperoxidation of the C_{31} botryococcene in an oxic environment followed by heterolytic (Hock-type) and homolytic cleavages around the quaternary carbon and subsequent hydrogenation is proposed to be the most likely pathway for the formation of the saturated C_{15} and C_{18} ketones.

Declaration of Competing Interest

The authors declared that there is no conflict of interest.

Acknowledgements

The authors thank Wenbin Zhang for their technical help with pGC instrumentation. HL acknowledges the financial support from The National Key R&D Program of China (2017YFC0603102)), The Strategic Priority Research Program of the Chinese Academy of Sciences (XDA14010102), The GIG-135 Shale Gas Project, China (135TP201602), National Major Equipment Grants of China [2017ZX05008-002-030], Project of State key laboratory of organic geochemistry of China (SKLOG2016-A02, SKLOG2016-A08) and Chinese NSF grants (41973069, 41673066, 41673045); YZ acknowledges the support of a Chinese NSF grant (41773032); JL acknowledges the support of a Chinese NSF grant (41903064). We thank the Chief Editor Professor Steven Rowland, the Associate Editor and two anonymous reviewers for their very helpful comments which greatly improved the manuscript. This is contribution No. IS-2765 from GIGCAS and # 11 from the Isotopomics in Chemical Biology group. Prof CH Hocart is gratefully acknowledged for improving the English of this manuscript.

Appendix A. Supplementary material

Supplementary data to this article can be found online at https://doi.org/10.1016/j.orggeochem.2019.103946.

Associate Editor—**George Andrew Wolf**

References

Aasen, A.J., Nishida, T., Enzell, C.R., Devreux, M., 1976. Tabacco Chemistry 37. Acta Chemica Scandinavica B30, 178.

Brassell, S.C., Eglinton, G., Fu, J.M., 1986. Biological marker compounds as indicators of the deposition history of the Maoming oil shale. Organic Geochemistry 10, 927–941.

Breitmaier, E., Voelter, W., 1978. 13C Nuclear Magnetic Resonance: Methods and Applications, Second Edition. Monographs in Modern Chemistry 5. Verlag Chemie.

Bigley, D.B., Clarke, M.J., 1982. Studies in decarboxylation. Part 14. The gas-phase decarboxylation of but-3-enoic acid and the intermediacy of isocrotonic (cis-but-2-enoic) acid in its isomerisation to crotonic (trans-but-2-enoic) acid. Journal of the Chemical Society, Perkin Transactions 2, 1–6.

Cheng, H.N., Bennett, M.A., 1991. Trends in shift rules in carbon-13 nuclear magnetic resonance spectroscopy and computer-aided shift prediction. Analytica Chimica Acta 242, 43–56.

Cheng, H.N., 1994. ^{13}C NMR spectral simulation and shift prediction. TrAC Trends in Analytic Chemistry 13, 95–104.

Deming, J.W., Baross, J.A., 1993. The early diagenesis of organic matter: bacterial activity. In: Engel, M.H., Macko, S.A. (Eds.), Organic Geochemistry. Plenum Press, New York, pp. 119–144.

Eglinton, T.I., Aluwihare, L.I., Bauer, J.E., Druffel, E.R.M., McNichol, A.P., 1996. Gas chromatographic isolation of individual compounds from complex matrices for radiocarbon dating. Analytical Chemistry 68, 904–912.

Frimer, A.A., 1979. The reaction of singlet oxygen with olefins: the question of mechanism. Chemical Review 79, 359–387.

Hinrichs, S.M., 1993. Early diagenesis of organic matter: the dynamics (rates) of cycling of organic compounds. In: Engel, M.H., Macko, S.A. (Eds.), Organic Geochemistry. Plenum Press, New York, pp. 101–117.

Jin, J., Hanefeld, U., 2011. The selective addition of water to C [double bond, length as m-dash] C bonds; enzymes are the best chemists. Chemical Communications 47, 2502–2510.

Liao, J., Lu, H., Feng, Q., Zhou, Y.P., Shi, Q., Peng, P.A., Sheng, G.Y., 2018a. Identification of a novel C_{33} botryococcane and C_{33} botryococcanone in the Maoming Basin, China. Organic Geochemistry 124, 103–111.

Liao, J., Lu, H., Feng, Q., Zhou, Y.P., Shi, Q., Peng, P.A., Sheng, G.Y., 2018b. Two novel decamethyl henicosanes ($C_{31}H_{64}$) identified in a Maoming Basin shale, China. Organic Geochemistry 125, 212–219.

Liao, J., Lu, H., Feng, Q., Zhou, Y.P., Shi, Q., Peng, P.A., Sheng, G.Y., ao et al., in preparation. Identification of a novel undecamethyl henicosane and three oxygenated precursors in a Maoming Basin shale, China. Organic Geochemistry.

Lindeman, L.P., Adama, J.Q., 1971. Carbon-13 nuclear magnetic resonance spectrometry. Chemical shifts for the paraffins through C_9. Analytical Chemistry 43, 1245–1252.

Mösle, B., Collinson, M.E., Finch, P., Stankiewicz, B.A., Scott, A.C., Wilson, R., 1998. Factors influencing the preservation of plant cuticles: a comparison of morphology and chemical composition of modern and fossil examples. Organic Geochemistry 29, 1369–1380.

Olah, G.A., Parker, D.G., Yoneda, N., Pelizza, F., 1976. Oxyfunctionalization of hydrocarbons. I. Protonic cleavage-rearrangement reactions of tertiary alkyl hydroperoxides with magic acid. Journal of the American Chemical Society 98, 2245–2250.

Resch, V., Hanefeld, U., 2015. The selective addition of water. Catalysis Science & Technology 5, 1385–1399.

Rontani, J.F., Bonin, P., Giusti, G., 1987. Mechanistic study of interactions between photo-oxidation and biodegradation of *n*-nonylbenzene in seawater. Marine Chemistry 22, 1–12.

Rontani, J.F., Giusti, G., 1988. Photosensitized oxidation of phytol in seawater. Journal of Photochemistry and Photobiology A: Chemistry 42, 347–355.

Rontani, J.F., Belt, S.T., Vaultier, F., Brown, T.A., 2011. Visible light induced photo-oxidation of highly branched isoprenoid (HBI) alkenes: significant dependence on the number and nature of double bonds. Organic Geochemistry 42, 812–822.

Rontani, J.F., 2012. Photo-and free radical-mediated oxidation of lipid components during the senescence of phototrophic organisms. In Senescence. IntechOpen.

Rontani, J.F., Volkman, J.K., Prahl, F.G., Wakeham, S.G., 2013. Biotic and abiotic degradation of alkenones and implications for UK′ 37paleoproxy applications: a review. Organic Geochemistry 59, 95–113.

Simoneit, B.R.T., Xu, Y., Neto, R.R., Cloutier, J.B., Jaffé, R., 2009. Photochemical alteration of 3-oxygenated triterpenoids: implication for the origin of 3,4-secotriterpenoids in sediments. Chemosphere 74, 543–550.

Wheeler, J.R., 1972. Some effects of solar levels of ultraviolet radiation on lipids in artificial seawater. Journal of Geophysical Research 77, 5302–5306.

Zhang, X.Y., Lu, H., Liao, J., Tang, C.M., Sheng, G.Y., Peng, P.A., 2017. Two new oxygen-containing biomarkers isolated from the Chinese Maoming oil shale by silica gel column chromatography and preparative gas chromatography. Journal of Separation Science 40, 813–818. now retracted.

Zuo, H.L., Yang, F.Q., Huang, W.H., Xia, Z.N., 2013. Preparative gas chromatography and its applications. Journal of Chromatographic Science 51, 704–715.